Front. Earth Sci. 2017, 11(2): 397–406
DOI 10.1007/s11707-016-0587-y

RESEARCH ARTICLE

Scale-location specific relations between soil nutrients and topographic factors in the Fen River Basin, Chinese Loess Plateau

Hongfen ZHU, Rutian BI (✉), Yonghong DUAN, Zhanjun XU

College of Resource and Environment, Shanxi Agricultural University, Shanxi 030801, China

Abstract Understanding scale- and location-specific variations of soil nutrients in cultivated land is a crucial consideration for managing agriculture and natural resources effectively. In the present study, wavelet coherency was used to reveal the scale-location specific correlations between soil nutrients, including soil organic matter (SOM), total nitrogen (TN), available phosphorus (AP), and available potassium (AK), as well as topographic factors (elevation, slope, aspect, and wetness index) in the cultivated land of the Fen River Basin in Shanxi Province, China. The results showed that SOM, TN, AP, and AK were significantly inter-correlated, and that the scales at which soil nutrients were correlated differed in different landscapes, and were generally smaller in topographically rougher terrain. All soil nutrients but TN were significantly influenced by the wetness index at relatively large scales (32–72 km) and AK was significantly affected by the aspect at large scales at partial locations, showing localized features. The results of this study imply that the wetness index should be taken into account during farming practices to improve the soil nutrients of cultivated land in the Fen River Basin at large scales.

Keywords soil nutrients, wavelet coherency, wetness index, spatial variation, cultivated land

1 Introduction

Soil organic matter (SOM), total nitrogen (TN), available phosphorus (AP), and available potassium (AK) are indicators of soil fertility which play a crucial role in plant growth in cultivated lands. The natural contents of soil nutrients are influenced by soil-forming processes, which are controlled by climate, topography, parent material, vegetation, and biotic factors (Jenny, 1941). Topography, which is controlled by drainage, runoff, and soil erosion, may affect the transposition and re-distribution of soil nutrients along the surface (Umali et al., 2012), so topographic factors including elevation, slope gradients, aspect, and wetness index can characterize these flow paths and variability of soil nutrients (Moore et al., 1993).

Certain controlling factors (e.g., microtopography) of soil nutrients may operate at short distances, while others (e.g., meteorological conditions) are likely to operate at larger scales (Holmes et al., 2005). To this effect, the influences of topographic factors on soil nutrients may be site-specific and scale-dependent. Due to complex combinations of human activity and natural processes, however, the location- and scale-dependent relationships among soil nutrients and environmental factors are highly complex – especially in cultivated lands. For efficient, effective, and environmentally responsible agricultural management, it is necessary to establish a full understanding of the multi-scale influences of topographic factors on soil nutrients.

The linear model of co-regionalization (LMC) can decompose a system of spatial variability into several different components pertaining to different scales, and as such, has been widely used to examine scale-specific relations (Goulard and Voltz, 1992). For example, Holmes et al. (2005) examined the spatial correlations of soil nutrients (soil organic carbon, nitrogen, phosphorus, and potassium) with land cover and terrain attributes at four spatial scales. Liu et al. (2013) identified that soil nutrients (soil organic carbon, total nitrogen, and total phosphorus) are controlled by factors at both scales of 12 km and 84 km. While the LMC is able to identify the dominant scales of soil nutrients, it limits the number of separated spatial components and loses location-specific information.

Received October 28, 2015; accepted February 14, 2016

E-mail: sxndbrt@163.com

Wavelet coherency is a method of measuring the relationships between two spatial variables at different locations and scales (Grinsted et al., 2004; Si and Zeleke, 2005) that has been successfully used to elucidate the location- and scale-dependent relationships between two time or spatial series in soil water (Shu et al., 2008), soil saturated hydraulic properties (Si and Zeleke, 2005), and soil nitrous oxide emissions (Yates et al., 2007). The spatial relationships between soil water and environmental factors such as precipitation (Wu et al., 2002; Andreo et al., 2006), drought index (Tang and Piechota, 2009), and topography (Biswas and Si, 2011) have been explored via wavelet coherency, as well as the temporal impact of climate on carbon fluxes (Van Gorsel et al., 2013). To the best of our knowledge, there has been no previous study to use wavelet coherency to examine the scale- and location-specific control of topographic factors on soil nutrients.

The Fen River Basin, which is located in the eastern part of the Loess Plateau in China, is characterized by a complicated landform. Its cultivated land, which has suffered long-term tillage with an area of 11,591 km^2, accounts for one third of the total area of the basin and is the main production source of crops and vegetation of Shanxi Province. In effort to better and more comprehensively understand the spatial patterns of soil nutrients in the Fen River Basin cultivated lands, we aimed to explore the scale- and location- specific relationships between soil nutrients (SOM, TN, AP, and AK) and topographic factors for topsoil (0–20 cm).

2 Materials and methods

2.1 Site description

The study was conducted at the Fen River Basin (35°20′–39°00′ N latitude, 110°30′–113°32′ E longitude) in Shanxi Province, North China (Fig. 1). The Fen River is one of the largest tributaries of the Yellow River in its middle reach, joining the Yellow River in Hejing County. The river basin is bounded by Taihang Mountain to the east, and Lvliang Mountain to the west, which also forms the boundary between Yellow River and Fen River. The basin contains two large grabens: Taiyuan Graben in the upper reach, and Linfen Graben in the lower reach (Bureau, 1988); the Linshi highland, similar to a gorge, incises the two grabens (Yang, 1987). The highest elevation of the area is 2786 m in the north and the lowest is 240 m in the south. Located in the eastern Loess Plateau of China, the climate of the Fen River Basin is temperate and sub-humid, with mean annual temperature between 6°C and 13°C and mean annual precipitation of 450 mm (Geography, 1985). In this area, the landforms are usually capped by a thick layer of loess due to dust deposition during the Quaternary (Hu et al., 2005). According to the FAO-90 soil classification system (Nachtergaele et al., 2008), the major soil types in the basin are Calcaric Cambisols and Calcaric Fluvisols, which are highly alkaline.

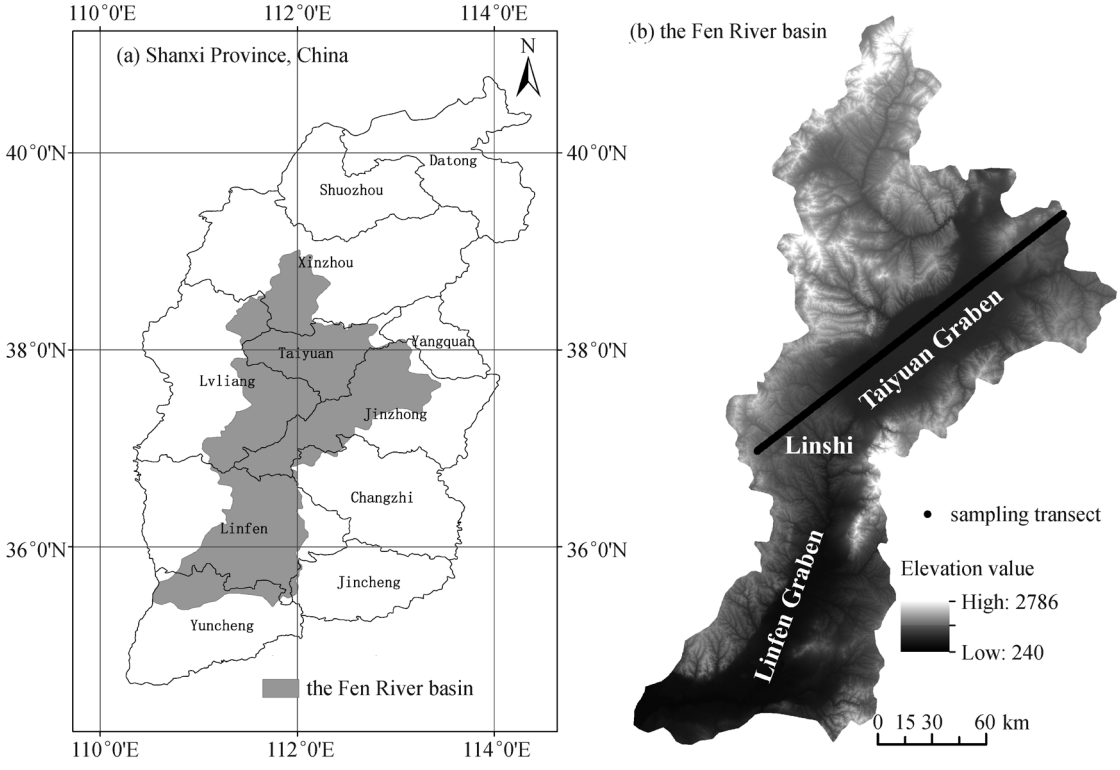

Fig. 1 Geographic location of study site and the extracted sampling location.

2.2 Data collection

For the purposes of this study, a total of 88,960 surface soil samples (0–20 cm) were taken in the Fen River Basin from 2002 to 2009. Soil nutrients including SOM, TN, AP, and AK were measured at each sampling location, all of which were geo-referenced with a global positioning system (GPS). The SOM content was determined by the Walkley and Black wet oxidation method (Page et al., 1982), TN was measured by the Kjeldahl method (Bremner et al., 1996), and AP was determined by the Olsen extraction method using alkaline sodium bicarbonate as the extractant in a 20:1 ratio (Olsen et al., 1954). AK was extracted using the ammonium acetate extraction method (Richards, 1947) and analyzed via flame photometer (Isaac and Kerber, 1972).

A subset of 18,143 sampling points from the total was extracted using a 1 km square fishnet of the Fen River Basin in ArcGIS 10.1 (ESRI Inc.). Interpolating images of soil nutrients in the Fen River Basin were obtained from the 18,143 soil samples by geostatistical method, also in ArcGIS. The root mean square errors (RMSEs) in the prediction models were 0.61 for SOM, 0.01 for TN, 0.90 for AP, and 5.63 for AK.

The sampling transect, with 215 points at 1 km intervals, was established from the 88,960 measured points across the Taiyuan Graben in a southwest-northeast direction, and elevation of the sampling transect went from 726 to 1395 m. If the nearest distance between an established point in the transect and a measured point was less than 500 m, the soil nutrients at that measured point represent that in the established point. Otherwise, the soil nutrients at the established points were extracted from the interpolating images of soil nutrients. There were 215 sampling points total in the established sampling transect, among which 198 points belonged to the measured points and 17 points were extracted from the interpolating images.

Topographic variables including elevation (related to climatic variables relevant to pedological processes), slope gradient (related to soil erosion and deposition), aspect (related to the amount of solar energy received by the soil surface), and wetness index (related to the redistribution of soil moisture in the landscape or soil erosion and accumulation) were selected for analysis. The digital elevation model (DEM) of the Fen River Basin (30 m resolution) was downloaded from an online resource (http://gdem.ersdac.jspacesystems.or.jp/) and used to derive the topographic indices for elevation, slope gradient, aspect, and wetness index.

2.3 Theory of wavelet coherency

Wavelet coherency was calculated from auto- and cross-wavelet power spectra, which require the calculation of wavelet coefficients at different scales and locations. The wavelet coherence of two spatial series (X and Y) was defined as follows (Torrence and Webster, 1999; Grinsted et al., 2004):

$$R_i^2(s) = \frac{|S(s^{-1}W_i^{XY}(s))|^2}{S(s^{-1}|W_i^X(s)|^2)S(s^{-1}|W_i^Y(s)|^2)}, \quad (1)$$

where, s is the scale, W_i^X and W_i^Y are the wavelet coefficients of the two spatial series (X and Y), W_i^{XY} is the cross wavelet power spectrum of the spatial series, and S is the smoothing operator. Further detail regarding wavelet coefficients, the cross wavelet power spectrum, and the smoothing operator can be found in the references (Torrence and Compo, 1998; Grinsted et al., 2004).

2.4 Data analysis

The soil sampling points were summarized and extracted and the images of soil nutrients (SOM, TN, AP, and AK) in the Fen River Basin were interpolated in ArcGIS 10.1. The established sampling transect of soil nutrients was obtained from the gathered soil sampling points and the interpolated images, and topographic factors (slope gradient, aspect, and wetness index) were calculated from the DEM developed in ArcGIS. Exploratory data analyses were implemented and graphs were prepared in Microsoft Excel 2007 (Microsoft Corporation, Inc.).

The wavelet coherency was completed with MATLAB code written by Grinsted et al. (2004). Following Si and Zeleke (2005), the relationships were considered spurious if the area with significant wavelet coherency (95% confidence level) was less than 5% of the total area. The total area of wavelet coherency between soil nutrients and between soil nutrients and topographic factors was 13,545 pixels (215 points × 63 scales), and the areas of these regions (95% confidence level and larger than 5% of the total area) were calculated accordingly to determine significantly correlated regions.

3 Results and discussion

3.1 Spatial pattern of soil nutrients

As shown in Table 1, the descriptive statistics of soil nutrients in the sampling transect were calculated. The mean values of SOM, TN, AP, and AK were 17.4 $g \cdot kg^{-1}$, 0.8 $g \cdot kg^{-1}$, 14.1 $mg \cdot kg^{-1}$, and 163.3 $mg \cdot kg^{-1}$, respectively, and the coefficients of variation (CV) values were 46.7%, 32.8%, 79.3%, and 43.9%, respectively. Based on previous reports, these variations can be considered moderate as the CV values were between 10% and 90% (Jiang et al., 2003; Zhang et al., 2007; Hu et al., 2008). The points in the sampling transect were mainly from a fairly brief time period, 2007 to 2008, so we assumed that temporal changes in soil nutrients were negligible compared to their spatial variations.

Table 1 Classical statistics of soil nutrients along the sampling transect

Soil nutrients	Mean	Max	Min	SD	CV/%	Skewness/(-)	Kurtosis/(-)
SOM/(g·kg^{-1})	17.4	54.0	3.2	8.1	46.7	1.6	3.5
TN/(g·kg^{-1})	0.8	1.7	0.1	0.3	32.8	0.5	1.5
AP/(mg·kg^{-1})	14.1	69.1	0.7	11.2	79.3	1.5	3.0
AK/(mg·kg^{-1})	163.3	457.0	66.0	71.6	43.9	1.6	3.4

SOM: soil organic matter; TN: total nitrogen; AP: available phosphorus; AK: available potassium; SD: standard deviation; CV: coefficient of variation.

Spatial distributions of the soil nutrients (SOM, TN, AP, and AK) and topographic factors (elevation, slope, aspect, and wetness index) are shown in Fig. 2. In the depression ranging from 60 km to 160 km, values and variations of wetness index were greater than other locations; this corresponded with greater variations of SOM, AP, and AK in the depression.

Scale-location specific variations in soil nutrients can be determined based on their local wavelet spectra (Fig. 3), which is the squared wavelet coefficient at each scale at each location. In the spectra we drew, as is typical, dark red colors are associated with higher wavelet variance, while dark blue colors are associated with lower wavelet variance. The thick contour enclosed regions indicate 95% confidence level for the corresponding local wavelet spectrum, which were established by the Monte Carlo method (Torrence and Compo, 1998). The global wavelet spectrum, indicating the wavelet power spectrum of soil nutrients at various scales along the sampling transect, is also shown in Fig. 3. The wavelet power spectrum used to measure the contribution of variance at a specific scale to the total variance was derived from the local wavelet coefficients (Si and Farrell, 2004). Solid lines in the global wavelet spectrum graph mark the variance of soil nutrients, which was plotted by averaging the local wavelet spectra over all locations; dashed lines are the variance at the 95% confidence level obtained via reshuffling method (Si, 2008).

Upon visual inspection, the patterns of spatial variance for SOM, AP, and AK were very similar according to the local wavelet spectra for soil nutrients (Fig. 3(a), 3(c) and 3 (d)). There were three scales of variation across the transect: 0–8 km, 8–32 km, and 32–72 km, referring to small, medium, and large scales, respectively. The region at the 0–8 km scale had mostly relatively small variances, but small regions with significantly high variances. For the scales of 8–32 km, the soil nutrient variances were relatively uniform and small, indicating variances of medium scale in the soil nutrients were small. At the scales of 32–72 km, variances were high. Regions with high variance (95% confidence level) were identified around the depression, and significant regions for SOM, AP, and AK were more obvious. However, the area of significant region for TN at the scales of 32–72 km was small, indicating the variation was not large.

The global wavelet spectrum revealed that spatial variations in AP and AK were similar (Figs. 3(c) and 3 (d)). There was a peak around 32–72 km in the global variance of AP and AK, indicating large variances in

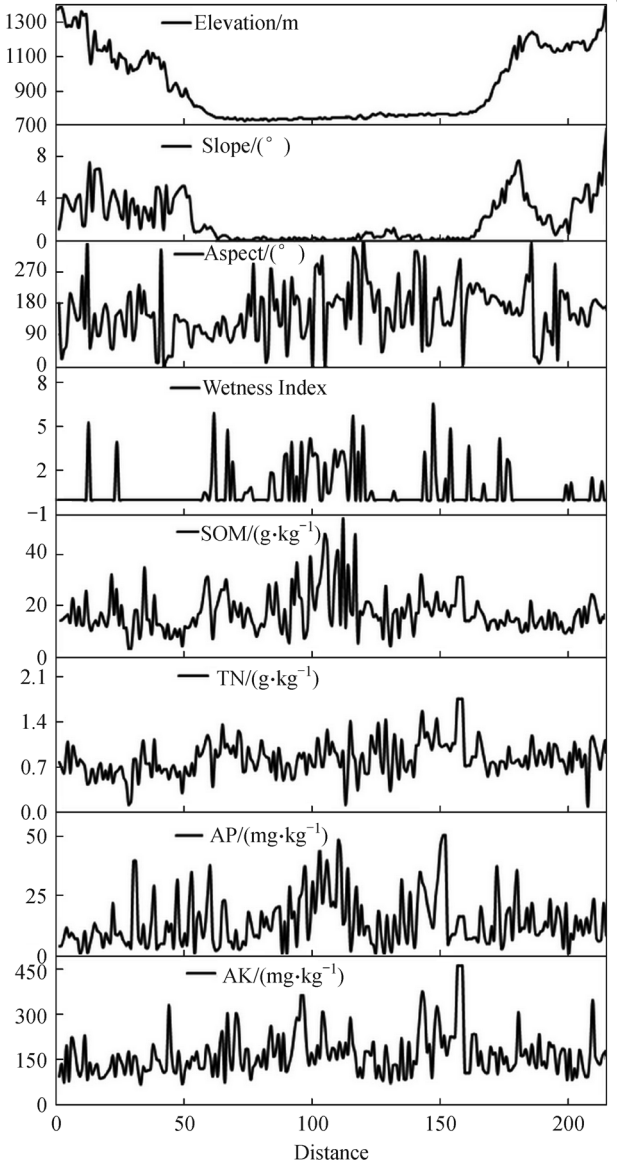

Fig. 2 Distribution of SOM, TN, AP, and AK with topographic factors of elevation, slope, aspect, and wetness index along the transect. SOM: soil organic matter; TN: total nitrogen; AP: available phosphorus; AK: available potassium.

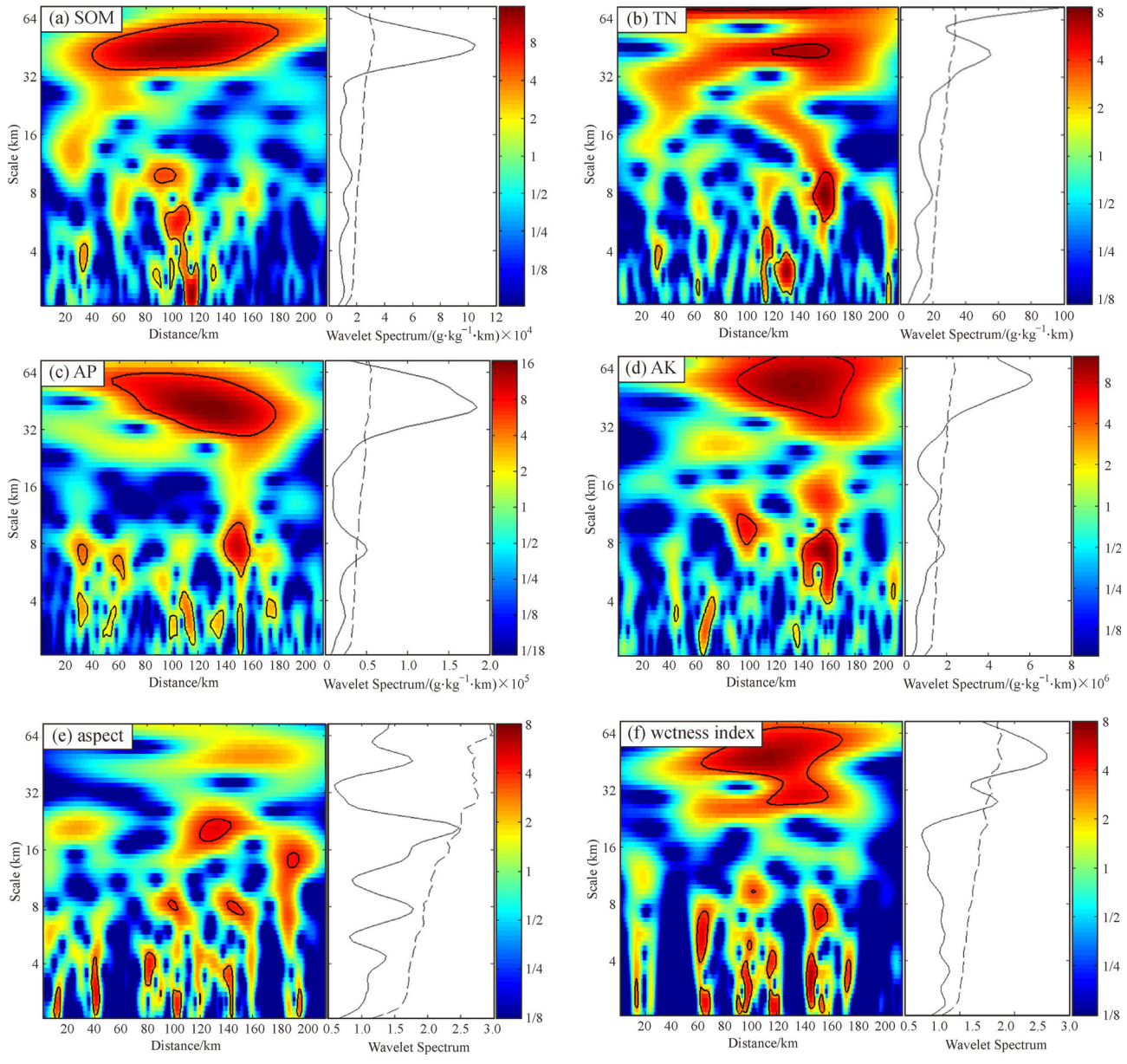

Fig. 3 Local (image) wavelet spectrum and global (graph) wavelet power spectrum of soil nutrients, and (a) SOM, (b) TN, (c) AP, (d) AK, (e) aspect and (f) wetness index. For the local wavelet spectrum, X-axis indicates distances along the sampling transect in km, Y-axis indicates scales in km, solid black line indicates 95% significance level, and the color bar indicates strength of variance. For the global wavelet spectrum, X-axis indicates wavelet power spectrum of each scale, Y-axis indicates scale in km, solid line indicates the variance of soil nutrients and dashed line indicates the variance in a confidence level of 95%. SOM: soil organic matter; TN: total nitrogen; AP: available phosphorus; AK: available potassium.

general, in addition to a smaller peak around 0–8 km suggesting that variances were high at the small scale as well. The variances of SOM and TN at scales < 32 km were relatively stable and small (Figs. 3(a) and 3(b)) and at 32–72 km, there was a dominant peak for SOM indicating significant variation, then two peaks for TN and an overall trend of higher variance at scales >72 km. This indicated that the most significant variances for TN were at scales>32 km, and that variance at scales of >72 km was the largest.

The local and global wavelet spectra of SOM, AP, and AK indicated that the operating scales of influencing factors were around 32–72 km. In terms of aspect, the local and global wavelet spectra showed there was no significant variance at any of the scales of 0–72 km (Fig. 3(e)), suggesting that the effect of aspect on soil nutrients is unpredictable. The spatial distribution of the wetness index (Fig. 3(f)) was very similar to SOM, AP, and AK, and the

variability at large scales of 32–72 km was stable, suggesting that wetness index likely plays a role in the spatial distribution of soil properties at large scales.

3.2 Wavelet coherency between soil nutrients

The scale- and location- specific correlation between soil nutrients was examined via wavelet coherency. As shown in Fig. 4 and Table 2, wavelet coherency analysis revealed significant correlation among soil nutrients in accordance with previous studies (Guo and Wang, 2013). There was significant correlation between SOM and TN, and the area of the three regions of significant wavelet coherency (at 95% confidence level and area larger than 5% of the total area) were 12.7% at scales 0–25 km and locations 0–87 km, 16.5% at scales 0–16 km and locations 127–215 km, and 5.6% at scales 28–45 km and locations 12–152 km, respectively. This indicated that the correlating scales vary by landform.

Our results suggested that the correlating scales were small and the variations large when the landform was complex (locations from 0 to 60 km and from 160 to 215 km) while the correlating scales were large and variations stable when the landform was simple (particu-

Table 2 The area of regions with significant wavelet coherency (in 95% confidence level and area larger than 5% of the total area) among soil nutrients

	Area/(pixels)	Area/%	Type of correlation	Scale/km	Location/km
SOM-TN	1717	12.7	Positive	0–25	0–87
	765	5.6	Positive	28–45	12–152
	2232	16.5	Positive	0–16	127–215
SOM-AP	1316	9.7	Positive	34–60	49–208
SOM-AK	1538	11.4	Positive	45–72	1–215
TN-AP	1769	13.1	Mostly positive	5–45	1–215
TN-AK	1007	7.4	Positive	0–17	116–174
	1280	9.5	Positive	18–48	80–215
AP-AK	1903	14.0	Positive	23–57	1–215

SOM: soil organic matter; TN: total nitrogen; AP: available phosphorus; AK: available potassium.

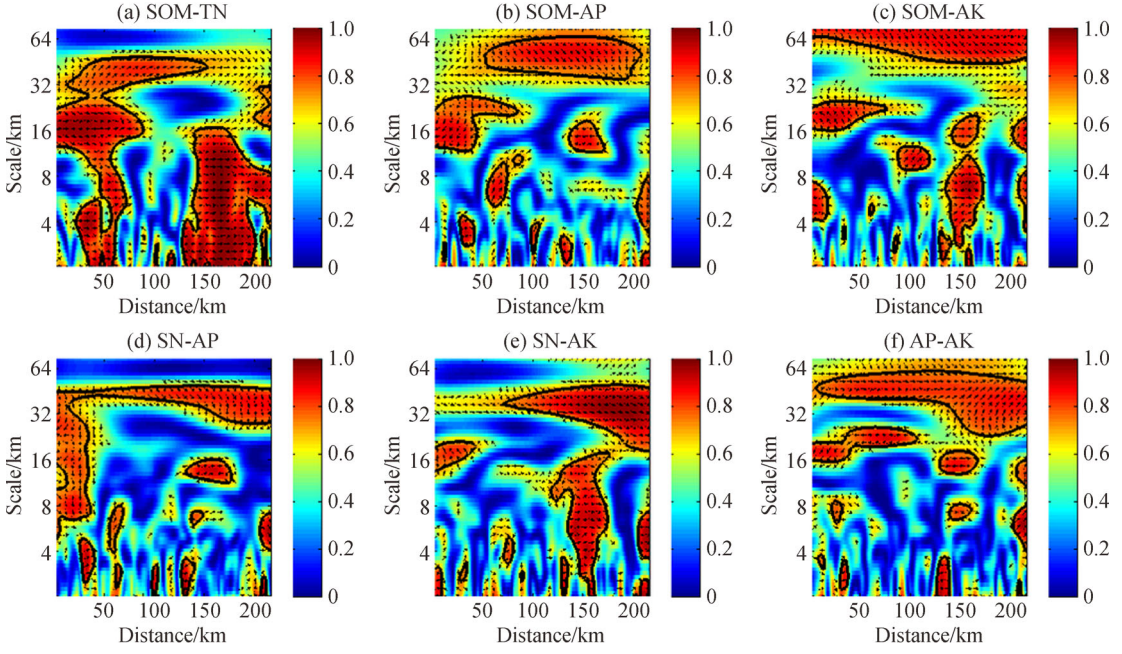

Fig. 4 Wavelet coherency between soil nutrients, (a) SOM with TN, (b) SOM with AP, (c) SOM with AK, (d) TN with AP, (e) TN with AK and (f) AP with AK. X-axis indicates distance along the sampling transect in km, Y-axis indicates scale in km, solid black line indicates 95% significance level, color bar indicates strength of correlation, and direction of arrow indicates the type of correlation (right direction- positive; left direction- negative). SOM: soil organic matter; TN: total nitrogen; AP: available phosphorus; AK: available potassium.

larly around the depression, from 60 to 160 km). The area of the significant region between SOM and AP was 9.7% at scales 34–60 km and locations 49–208 km, suggesting close correlation between SOM and AP in the depression. The correlating scale of SOM with AP was 34–60 km, where the dominant variance contributions were similar and located at large scales, 32–72 km (Figs. 3(a) and 3(c)). The area of the significant region between SOM and AK was 11.4% at scales 45–72 km at all locations and grew wider from 0–215 km, indicating that the correlation between SOM and AK was also related to the specific landform. Additionally, the correlating scale between SOM and AK was 45–72 km at the large scale (32–72 km), comprising the dominant variance contribution of SOM and AK.

The area of the significant region between TN and AP was 13.1% at scales 5–45 km at all locations. At medium scale (8–32 km), TN was significantly correlated with AP at the more complicated landforms, especially at 0–50 km locations. At scales of 32–45 km, TN had a significant relationship with AP at all locations, indicating that the correlating scale of TN and AP was around 40 km and had close correlation at medium scale, even in complex landforms. The area of the significant region between TN and AK were 9.5% at scales 18–48 km and locations 80–215 km, and 7.4% at scales 0–17 km and locations 116–174 km, suggesting that correlating scales between TN and AK varied by landform. For TN and AK, the correlation was not significant at the complicated landform (0–50 km), but was significant at medium scales (18–48 km). The correlating scale varied even in the depression, where the landform was much simpler. Basically, the relationship between TN and AK was complicated along the transect according to different landscapes.

The area of the significant region between AP and AK was 14.0% at scales 23–57 km at all locations while the shape of correlating regions along the transect were different, which may suggest that the relationship between AP and AK was stable regardless of landform except for 160–215 km locations.

The types of correlation were shown by the direction of the arrow; right arrow indicated positive correlation and left arrow indicated negative correlation. It is clear that all correlations were positive at significantly correlating regions (95% confidence level and area larger than 5% of the total area), except for TN and AP, which were not stable at locations 0–50 km (Fig. 4). The different types of correlation between TN and AP at locations 0–50 km may have been due to the complicated landform and unstable variations in TN and AP at scales 5–32 km.

3.3 Wavelet coherency among soil nutrients and topographic Factors

Significant coherences were identified between each soil nutrient (SOM, AP, and AK) and the wetness index, and between AK and aspect (Fig. 5). The percentage areas of significant wavelet coherence are listed in table 3. The

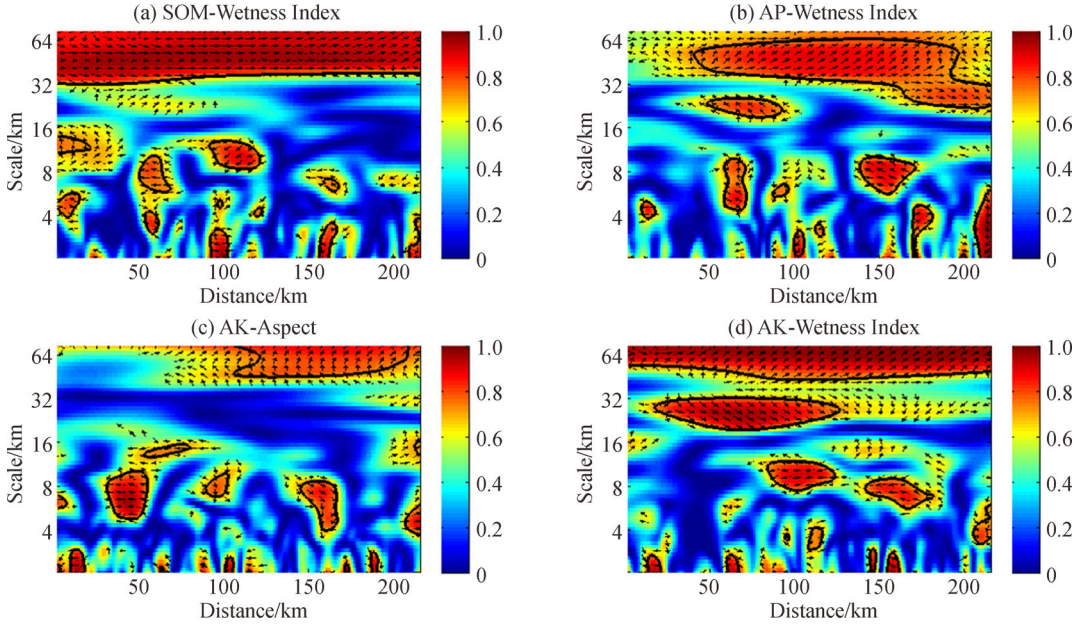

Fig. 5 Wavelet coherency of soil nutrients with topographic parameters, (a) SOM with Wetness Index, (b) AP with Wetness Index, (c) AP with Aspect, and (d) AK with Wetness Index. X-axis indicates distance along the sampling transect in km, Y-axis indicates scale in km, solid black line indicates 95% significance level, color bar indicates strength of correlation, and direction of arrow indicates the type of correlation (right direction- positive; left direction- negative). SOM: soil organic matter; AP: available phosphorus; AK: available potassium.

Table 3 The area of regions with significant wavelet coherency (in 95% confidence level and area larger than 5% of the total area) between soil nutrients and topographic factors.

	Area/pixels	Area/%	Type of correlation	Scale/km	Location/km
SOM-Wetness Index	2796	20.6	Positive	32–72	1–215
AP-Wetness Index	1824	13.5	Positive	23–60	39–215
AK-Aspect	822	6.1	Positive	45–72	98–215
AK-Wetness Index	1688	12.5	Positive	45–72	1–215
	702	5.2	Positive	19–30	16–126

SOM: soil organic matter; TN: total nitrogen; AP: available phosphorus; AK: available potassium.

distribution of SOM content was more stable at scales < 32 km, and was not affected by the topographic factors analyzed apart from the wetness index, which had a positive effect on SOM at scales 32–72 km at all locations (Fig. 5). Previous studies have reached similar conclusions (Hu et al., 2015; Luca et al., 2007; Sumfleth and Duttmann, 2008). It is likely that wetter soil could increase SOM content by benefiting plant growth and slowing down SOM decomposition (Pei et al., 2010; Starr et al., 2000). The significantly correlated scale of SOM with the wetness index also agreed with the scale of stable variance for SOM (Fig. 3), and none of the correlating locations of SOM with the wetness index were associated with any particular landscape or location.

TN was not affected by any topographic factors in the cultivated land of the Fen River Basin, which might be attributed to the frequent use of nitrogenous fertilizers in the region. The spatial TN was more influenced by anthropogenic activity than by topographic features. The local and global wavelet spectra of TN revealed that the scales of the largest dominant variance were >72 km (Fig. 3(b)), indicating that the influencing factors of TN are prevalent at >72 km.

Variability of AP was not influenced by elevation, slope, or aspect, possibly because phosphorus is minimally soluble especially in alkaline and calcareous soils. Therefore, it is likely that AP is not readily affected by environmental factors but instead by farming practices (Hopkins and Ellsworth, 2005). AP was, however, positively correlated with the wetness index at scales 23–60 km and locations 39–215 km (Fig. 5). The region of significant wavelet coherency could be divided into three parts: locations 39–160 km, 160–200 km, and 200–215 km. The region from 39 to 160 km was mainly at larger scale (32–60 km) in accordance with the spatial variation of AP (Fig. 3(c)). The region located from 160 to 200 was at scale 23–60 km, and at >200 km was at scale 23–32 km, which may be attributable to the complex landforms at these locations. Similar to TN, the long-term tillage and phosphate fertilization in cultivated lands affected total phosphorous content. The significant correlation between AP and the wetness index might be attributed to the wetness index affecting biological activity which affects the availability of phosphorus (Saleque et al., 1996; Keith et al., 1997).

Soil AK was positively affected by the wetness index at scales 45–72 km at all locations and at scales 19–30 km at locations 16–126 km (Fig. 5). AK was also positively influenced by aspect at scales 45–72 km and locations 98–215 km, because potassium is a highly mobile ion and easily leached from the ecosystem (Kolahchi and Jalali, 2007), and as such is readily affected by environmental factors. The dominant region for AK with the wetness index was at the large scale (32–72 km), similar to the scale of stable variation for AK and the wetness index, the exception being the significant region from 16 to 126 km at medium scale (19–30 km). These observations were likely due to the fact that the landform at this location was complicated and the operating scales of the wetness index to AK were at medium and large scale. The correlation between AK and wetness index was not related to any specific landform at large scale, but did differ by landform at medium scale. The effect of aspect on AK appeared unpredictable due to unstable variance of aspect at all scales observed.

In short, SOM, AP, and AK were all significantly influenced by the wetness index. The correlation of the wetness index with soil nutrients may be attributed to the fact that the wetness index is characterized by pedogenic processes such as soil erosion and accumulation or redistribution of soil moisture in the landscape (Moore et al., 1993; Beguería et al., 2013). The soil in the Fen River is some of the most highly erodible on Earth due to its location in the Loess Plateau, thus, its nutrients are readily affected by the comprehensive topographic wetness index. However, there were not any correlations between TN and topographic factors, which may be due to the tillage practice of frequent nitrogenous fertilizer use in the region. The dominant correlations of soil nutrients with the wetness index were mainly at large scale, 32–72 km, in accordance with the significant spatial variance between the wetness index and soil nutrients. In effect, the wetness index controlled the spatial variance of SOM, TN, and AK at scales 32–72 km. In addition, correlations existed at all locations at large scales with the sole exception of correlation between AP and the wetness index, suggesting

that correlations were not particularly affected by landscape at scales 32–72 km.

4 Conclusions

In this study, wavelet coherency analysis was used to explore the location- and scale-specific relationships between soil nutrients and topographic factors in the cultivated land of the Fen River Basin, China. Wavelet coherency revealed that the relationships between any two soil nutrients were very strong and the correlations among them were specific to both location and scale. Meanwhile, the wetness index affected SOM and AK positively at the large scale at all locations, and affected AP at the large scale at locations 39–215 km. AK was positively affected by aspect, though in an unstable manner, and TN was not affected by any topographic factor. It indicated that the wetness index, which is related to pedogenic processes, should be a primary concern in the spatial distribution of soil nutrients at large scales (32–72 km). Because the large graben is highly representative of the entire Loess Plateau, these results can be extended to wider areas with similar topographic properties to help agricultural managers, researchers, and developers to better understand and account for the spatial distribution of soil nutrients in cultivated lands.

Acknowledgements This research was supported by the Innovation Grant of Shanxi Agricultural University (2014009), Shanxi Programs for Science and Technology Development of China (20120311009-1), and the National Natural Science Foundation of China (Grant No. 51304130). The authors declared that they have no conflicts of interest to this work.

References

Andreo B, Jiménez P, Durán J J, Carrasco F, Vadillo I, Mangin A (2006). Climatic and hydrological variations during the last 117–166 years in the south of the Iberian Peninsula, from spectral and correlation analyses and continuous wavelet analyses. J Hydrol (Amst), 324(1–4): 24–39

Beguería S, Spanu V, Navas A, Machín J, Angulo-Martínez M (2013). Modeling the spatial distribution of soil properties by generalized least squares regression: toward a general theory of spatial variates. J Soil Water Conserv, 68(3): 172–184

Biswas A, Si B C (2011). Identifying scale specific controls of soil water storage in a hummocky landscape using wavelet coherency. Geoderma, 165(1): 50–59

Bremner J, Sparks D, Page A, Helmke P, Loeppert R, Soltanpour P, Tabatabai M, Johnston C, Sumner M (1996). Nitrogen-total. Methods of soil analysis. Part 3-chemical methods, 1085–1121

Bureau RG o S S (1988). Active Fault System Around Ordos Massif. Beijing: Seismoic Press (in Chinese)

Geography EB o C s P (1985). Physical Geography of China.Beijing: General Science Press (in Chinese)

Goulard M, Voltz M (1992). Linear coregionalization model: tools for estimation and choice of cross-variogram matrix. Math Geol, 24(3): 269–286

Grinsted A, Moore J C, Jevrejeva S (2004). Application of the cross wavelet transform and wavelet coherence to geophysical time series. Nonlinear Process Geophys, 11(5/6): 561–566

Guo Z, Wang D (2013). Long-term effects of returning wheat straw to croplands on soil compaction and nutrient availability under conventional tillage. Plant Soil Environ, 59(6): 280–286

Holmes K W, Kyriakidis P C, Chadwick O A, Soares J V, Roberts D A (2005). Multi-scale variability in tropical soil nutrients following land-cover change. Biogeochemistry, 74(2): 173–203

Hopkins B, Ellsworth J (2005). Phosphorus availability with alkaline/calcareous soil. Western Nutrient Management Conference, 6, 88–93

Hu W, Chau H W, Si B C (2015). Vis‐near ir spectroscopy for soil organic carbon content measurement in the Canadian Prairies. CLEAN–Soil, Air. Water, 43(8): 1215–1223

Hu W, Shao M A, Wang Q J, Fan J, Reichardt K (2008). Spatial variability of soil hydraulic properties on a steep slope in the Loess Plateau of China. Scientia Agricola, 65(3): 268–276

Hu X, Li Y, Yang J (2005). Quaternary paleolake development in the Fen River Basin, North China. Geomorphology, 65(1–2): 1–13

Isaac E, Kerber J D (1972). Atomic absorption and flame photometry: techniques and uses in soil, plant and water analysis. SSSA

Jenny H (1941). Factors of Soil Formation.New York: McGraw-Hill Book Company

Jiang Y, Zhang Y, Wen D, Liang W (2003). Spatial heterogeneity of exchangeable iron content in cultivated soils of Shenyang suburbs. J Soil Water Conserv, 17(1): 277–289 (in Chinese)

Keith H, Jacobsen K, Raison R (1997). Effects of soil phosphorus availability, temperature and moisture on soil respiration in *Eucalyptus pauciflora* forest. Plant Soil, 190(1): 127–141

Kolahchi Z, Jalali M (2007). Effect of water quality on the leaching of potassium from sandy soil. J Arid Environ, 68(4): 624–639

Liu Y, Lv J, Zhang B, Bi J (2013). Spatial multi-scale variability of soil nutrients in relation to environmental factors in a typical agricultural region, Eastern China. Sci Total Environ, 450–451(0): 108–119

Luca C, Si B C, Farrell R E (2007). Upslope length improves spatial estimation of soil organic carbon content. Can J Soil Sci, 87(3): 291–300

Moore I D, Gessler P E, Nielsen G A, Peterson G A (1993). Soil attribute prediction using terrain analysis. Soil Sci Soc Am J, 57(2): 443–452

Nachtergaele F, Van Velthuizen H, Verelst L, Batjes N, Dijkshoorn K, Van Engelen V, Fischer G, Jones A, Montanarella L, Petri M (2008). Harmonized world soil database. Food and Agriculture Organization of the United Nations

Olsen S R, Cole C V, Watanabe F S (1954). Estimation of Available Phosphorus in Soils by Extraction with Sodium Bicarbonate. Washington: USDA

Page A, Miller R, Keeney D (1982). Total carbon, organic carbon, and organic matter. Methods of Soil Analysis, 2: 539–579

Pei T, Qin C Z, Zhu A, Yang L, Luo M, Li B, Zhou C (2010). Mapping soil organic matter using the topographic wetness index: a comparative study based on different flow-direction algorithms and

kriging methods. Ecol Indic, 10(3): 610–619

Richards L A (1947). Diagnosis and improvement of saline and alkaline soils. Soil Sci, 64(5): 432

Saleque M, Abedin M, Bhuiyan N (1996). Effect of moisture and temperature regimes on available phosphorus in wetland rice soils. Commun Soil Sci Plant Anal, 27(9–10): 2017–2023

Shu Q, Liu Z, Si B (2008). Characterizing scale-and location-dependent correlation of water retention parameters with soil physical properties using wavelet techniques. J Environ Qual, 37(6): 2284–2292

Si B C (2008). Spatial scaling analyses of soil physical properties: a review of spectral and wavelet methods. Vadose Zone J, 7(2): 547–562

Si B C, Farrell R E (2004). Scale-dependent relationship between wheat yield and topographic indices. Soil Sci Soc Am J, 68(2): 577–587

Si B C, Zeleke T B (2005). Wavelet coherency analysis to relate saturated hydraulic properties to soil physical properties. Water Resour Res, 41(11): W11424

Starr G, Lal R, Malone R, Hothem D, Owens L, Kimble J (2000). Modeling soil carbon transported by water erosion processes. Land Degrad Dev, 11(1): 83–91

Sumfleth K, Duttmann R (2008). Prediction of soil property distribution in paddy soil landscapes using terrain data and satellite information as indicators. Ecol Indic, 8(5): 485–501

Tang C, Piechota T C (2009). Spatial and temporal soil moisture and drought variability in the Upper Colorado River Basin. J Hydrol (Amst), 379(1–2): 122–135

Torrence C, Compo G P (1998). A practical guide to wavelet analysis. Bull Am Meteorol Soc, 79(1): 61–78

Torrence C, Webster P J (1999). Interdecadal changes in the ENSO-monsoon system. J Clim, 12(8): 2679–2690

Umali B P, Oliver D P, Forrester S, Chittleborough D J, Hutson J L, Kookana R S, Ostendorf B (2012). The effect of terrain and management on the spatial variability of soil properties in an apple orchard. Catena, 93(0): 38–48

Van Gorsel E, Berni J A J, Briggs P, Cabello-Leblic A, Chasmer L, Cleugh H A, Hacker J, Hantson S, Haverd V, Hughes D, Hopkinson C, Keith H, Kljun N, Leuning R, Yebra M, Zegelin S (2013). Primary and secondary effects of climate variability on net ecosystem carbon exchange in an evergreen Eucalyptus forest. Agric Meteorol, 182–183(0): 248–256

Wu W, Geller M A, Dickinson R E (2002). The response of soil moisture to long-term variability of precipitation. J Hydrometeorol, 3(5): 604–613

Yang J C (1987). The alluvial terraces and neotectonics in the south sector of the Fen River. In: Research Group of State Seismological Bureau, ed. The Tectonic Stress and Crust Structure. Beijing: Geology Press, 132–136 (in Chinese)

Yates T T, Si B C, Farrell R E, Pennock D J (2007). Time, location, and scale dependence of soil nitrous oxide emissions, soil water, and temperature using wavelets, cross-wavelets, and wavelet coherency analysis. J Geophys Res, D, Atmospheres, 112(D9): D09104

Zhang X Y, Sui Y Y, Zhang X D, Meng K, Herbert S J (2007). Spatial variability of nutrient properties in black soil of northeast China. Pedosphere, 17(1): 19–29